the plant journal

SEB SOCIETY FOR EXPERIMENTAL BIOLOGY

The Plant Journal (2023) **116,** 786–803 doi: 10.1111/tpj.16409

Comparative constraint-based modelling of fruit development across species highlights nitrogen metabolism in the growth-defence trade-off

Sophie Colombié[1,2,*], Sylvain Prigent[1,2], Cédric Cassan[1,2], Ghislaine Hilbert-Masson[3], Christel Renaud[3], Emilia Dell'Aversana[4], Petronia Carillo[4], Annick Moing[1,2], Chloé Beaumont[1], Bertrand Beauvoit[1], Tim McCubbin[5], Lars Keld Nielsen[5] and Yves Gibon[1,2]

[1]*Univ. Bordeaux, INRAE, UMR1332 BFP, 33882 Villenave d'Ornon, France,*

[2]*Bordeaux Metabolome, MetaboHUB, PHENOME-EMPHASIS, 33140 Villenave d'Ornon, France,*

[3]*EGFV, Université de Bordeaux, Bordeaux Sciences Agro, INRAE, ISVV, 33882 Villenave d'Ornon, France,*

[4]*Department of Environmental, Biological and Pharmaceutical Sciences and Technologies, University of Campania "Luigi Vanvitelli", Via Vivaldi 43, 81100 Caserta, Italy, and*

[5]*Australian Institute for Bioengineering and Nanotechnology (AIBN), The University of Queensland, Corner College and Cooper Roads (Building 75), Brisbane, QLD 4072, Australia*

Received 31 March 2023; revised 19 July 2023; accepted 21 July 2023; published online 2 August 2023.
*For correspondence (e-mail sophie.colombie@inrae.fr).

SUMMARY

Although primary metabolism is well conserved across species, it is useful to explore the specificity of its network to assess the extent to which some pathways may contribute to particular outcomes. Constraint-based metabolic modelling is an established framework for predicting metabolic fluxes and phenotypes and helps to explore how the plant metabolic network delivers specific outcomes from temporal series. After describing the main physiological traits during fruit development, we confirmed the correlations between fruit relative growth rate (RGR), protein content and time to maturity. Then a constraint-based method is applied to a panel of eight fruit species with a knowledge-based metabolic model of heterotrophic cells describing a generic metabolic network of primary metabolism. The metabolic fluxes are estimated by constraining the model using a large set of metabolites and compounds quantified throughout fruit development. Multivariate analyses showed a clear common pattern of flux distribution during fruit development with differences between fast- and slow-growing fruits. Only the latter fruits mobilise the tricarboxylic acid cycle in addition to glycolysis, leading to a higher rate of respiration. More surprisingly, to balance nitrogen, the model suggests, on the one hand, nitrogen uptake by nitrate reductase to support a high RGR at early stages of cucumber and, on the other hand, the accumulation of alkaloids during ripening of pepper and eggplant. Finally, building virtual fruits by combining 12 biomass compounds shows that the growth-defence trade-off is supported mainly by cell wall synthesis for fast-growing fruits and by total polyphenols accumulation for slow-growing fruits.

Keywords: constraint-based modelling; metabolic fluxes, fruit comparison, fruit development, primary metabolism, nitrogen and carbon metabolisms, multi-species.

INTRODUCTION

Plant genetic diversity, the basis for survival of plants in nature, is large within plant species. This diversity leads to various phenotypes and decoding the genetic basis of natural variation is central to understanding plant and especially crop evolution and, in turn, improving crop breeding (Liang et al., 2021). Plant growth and development are interwoven with primary metabolism and its regulation occurring at different levels, including gene expression, enzyme activity and metabolite abundance.

Major contributions about the analysis of natural variation of plant development and physiology highlighted genes involved in domestication traits (Perez-Roman et al., 2022), such as those related to plant architecture, fruit and seed structure and morphology, as well as yield and quality traits for crop plants and *Arabidopsis thaliana* (Alonso-Blanco et al., 2009). Natural variation has been

used to study growth traits (e.g., biomass accumulation, morphology), primary metabolism and mineral nutrition especially in the agronomical context. The complex molecular bases underlying these traits are beginning to be elucidated for hybrid vigour (positive heterosis), hybrid incompatibility (negative heterosis), and for specific metabolic pathways and physiological processes that affect crop growth and/or crop quality. Recently, molecular analyses of natural variation have identified enzyme-encoding genes and have associated plant metabolism with variations in morphological and developmental traits (Fang et al., 2018). Thus, metabolomics performed in genetically diverse populations facilitates the dissection of phenotypic traits and could lead to metabolite-assisted breeding.

From a process-based point of view, cross-species comparison can also help in comprehending physiological mechanisms. For instance, water-stress studied with three crops, maize, barley and rice, showed species diversity in terms of mechanisms of leaf growth inhibition. Indeed despite numerous inter-species similarities, the biophysical changes associated with stress-induced leaf growth inhibition in maize and barley, differed from those in rice (Lu & Neumann, 1998).

Fleshy fruits are highly diverse regarding their physiology, shape, colour, composition and growth duration. A better understanding of the mechanisms that link metabolism to phenotypes may help guide improved agronomical practices or breeding strategies. To our knowledge, few studies have been published about the comparison of fruit species (Roch et al., 2019). An inter-species comparison of three fruit species: grape, tomato and peach, focusing on sugar accumulation during fruit development allowed to identify the regulation modes in sugar accumulation using a process-based mathematical framework (Dai et al., 2016). More recently, sugar and starch accumulation strategies across 10 contrasting fruit species were compared with a process-based modelling approach (Cakpo et al., 2020). These authors showed that the coordination of metabolic processes involved in carbon allocation is shaped by the differences in fruit development period across fruit species. More interestingly, a comparative study of eight fruit species revealed a strong link between biomass composition and growth rate (Roch et al., 2020). More precisely, growth rate and growth duration were, respectively, greater and shorter in herbaceous plants than in trees or vines. The authors were not only able to discriminate the three fruit types, but also highlighted a set of relevant variables, in particular structural components such as proteins and cell wall polysaccharides.

Assuming that metabolism contributes to fruit growth we can expect to identify pathways or reactions with key roles regarding biomass construction. For this, the integration of experimental and modelling approaches allowing to compare the fluxes in the primary metabolic network of several species can be useful. Flux is one of the most informative measures of metabolic behaviour and flux analysis and modelling of a range of plant models point to the importance of the supply of metabolic inputs and demand for metabolic end-products as key drivers of metabolic behaviour (Sweetlove et al., 2014). To assess the rate of each reaction and to evaluate the dynamics of metabolism mainly based on carbon and nitrogen, metabolic flux analysis and constraint-based modelling allow to calculate fluxes in a metabolic model (see Clark et al., 2020a for recent review of plant modelling metabolism). Indeed, constraint-based modelling makes it possible to estimate fluxes even in very large models by using constraints to reduce the flux solution space. For model plants and crops, genome-scale metabolic networks combined with constraint-based modelling have been used to predict metabolic traits and design metabolic engineering strategies for their manipulation (Tong et al., 2021). These authors showed how constraint-based approaches that integrate genetic variants in genome-scale metabolic models are used to characterise their effects on reaction fluxes. Medium-scale models reconstructed from biochemical and bibliographic knowledge can satisfactorily describe the primary metabolism (Colombié et al., 2015) and in turn reveal unexpected behaviours such as a respiration peak occurring at the beginning of ripening due to an excess of carbon in the cell coming from starch and cell wall degradation (Colombié et al., 2017). It may also be useful to consider specialised or secondary metabolic pathways during modelling. For instance, in heterotrophic plant cells, anthocyanin biosynthesis was confirmed to act as an energy escape valve, thus opening new possibilities to manipulate flavonoid production (Soubeyrand et al., 2018).

However, the majority of modelling work is performed for one plant or fruit species, selected as a research model and for its economic interest (such as tomato or grape) and as far as we know there are no comparative studies of a panel of plant or fruit species using a metabolic modelling approach. Consequently in this work, to identify how metabolic pathways contribute to the biomass composition and to evaluate how metabolism contributes to growth rate, we estimated metabolic fluxes of primary metabolism of eight fleshy fruit species throughout fruit development, based on previous experimental results (Roch et al., 2020). Then, statistical analyses were used to compare fruit metabolic fluxes and identify key variables supporting fruit growth. This allowed us to answer simple but non-trivial questions. Which fruits require more carbon and energy, fruits from tree species that grow longer or those from herbaceous plants that grow faster? Does the fast construction of fruits of herbaceous plants require specific resources?

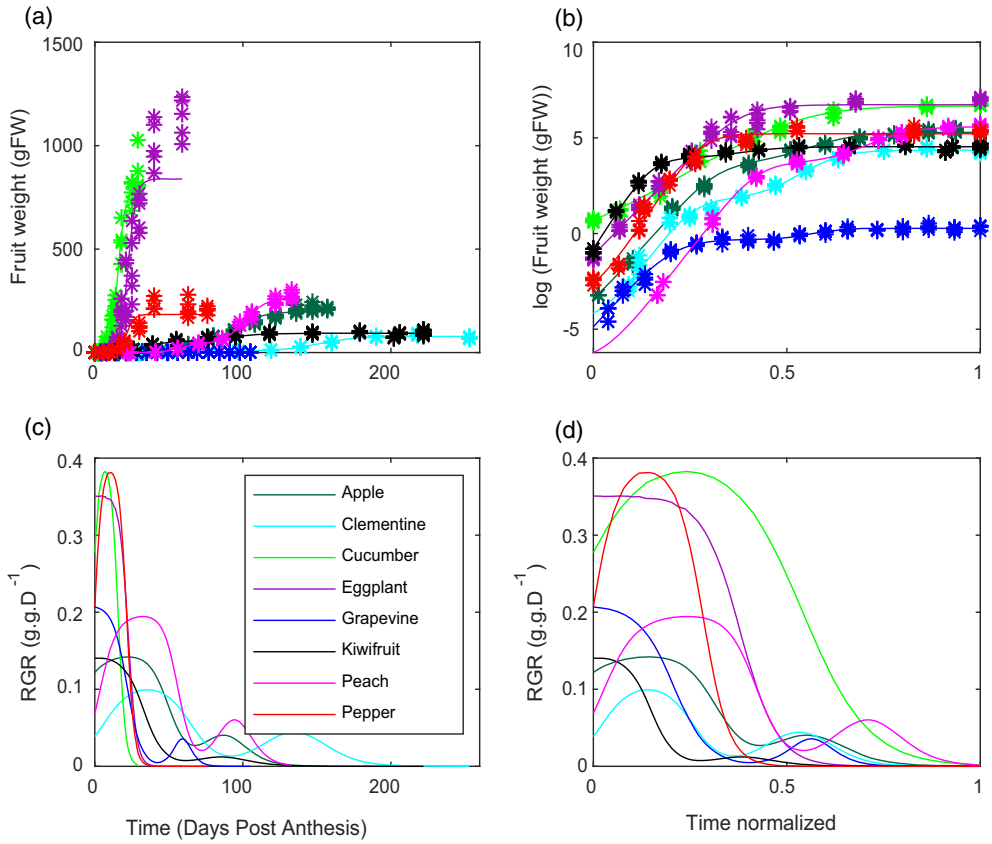

Figure 1. Time-course of (a, b) fruit fresh weight (g FW, stars) with the fit of growth (solid line) by sigmoid or double-sigmoid functions and (c, d) the corresponding relative growth rate (RGR, D^{-1}) throughout fruit development with absolute time on the left (in days post anthesis) and time normalised by the time to maturity on the right, in a panel of eight fruit species.

RESULTS

Time to maturity, relative growth rate and protein content are related in fruit

Eight fruit species, including three herbaceous species, that is, eggplant, pepper and cucumber, three tree species, i.e. apple, peach and clementine and two vine species, that is, kiwifruit and grape, were selected for their diversity. The changes in fruit biomass throughout development were previously modelled using sigmoid or double-sigmoid functions (Roch et al., 2020), which made it possible to calculate the growth rate and the relative growth rate (RGR) (Figure 1). For clarity, time was normalised by the time to maturity (Figure 1b,d). Interestingly, a linear relationship was found between the maximal value of RGR (RGR_{max}) and the time to maturity (between anthesis and ripeness). Strikingly, doubling time, which is a classic formula (Ln2/RGR) used to calculate the time needed for the doubling of a cell population, was strongly correlated to developmental time when RGR_{max} was used (Figure 2a). Since RGR_{max} occurs at the beginning of fruit development (Figure 1c,d), this suggests that cell division and/or cell expansion rates are important factors regarding time to maturity. As the fruits were grown under different temperature conditions, time-course of RGR were also plotted with time expressed in growing degree-days (GDD; Figure S1). Interestingly, RGR profiles of fruit from trees tend to get closer to each other and similar results were obtained with a significant relationship between the time to maturity expressed in GDD and RGR_{max} expressed as $Ln2/RGR_{max}$.

Protein content has been identified as the most predictive variable of RGR among the major components of fruit biomass (Roch et al., 2020). Interestingly, maximum protein content (expressed on a dry weight basis), which in most cases was measured in the ovary (Figure S3), was significantly correlated with RGR_{max} (Figure 2b; Figures S1 and S2). Furthermore, maximum protein concentration was always measured at the same time or before RGR_{max}, reinforcing the idea of a causal relationship (Table 1). Protein synthesis is costly in energy but also in nitrogen. To understand better the impact of protein synthesis among other major components of biomass, a modelling approach to compare the metabolic fluxes of eight fruit species was used.

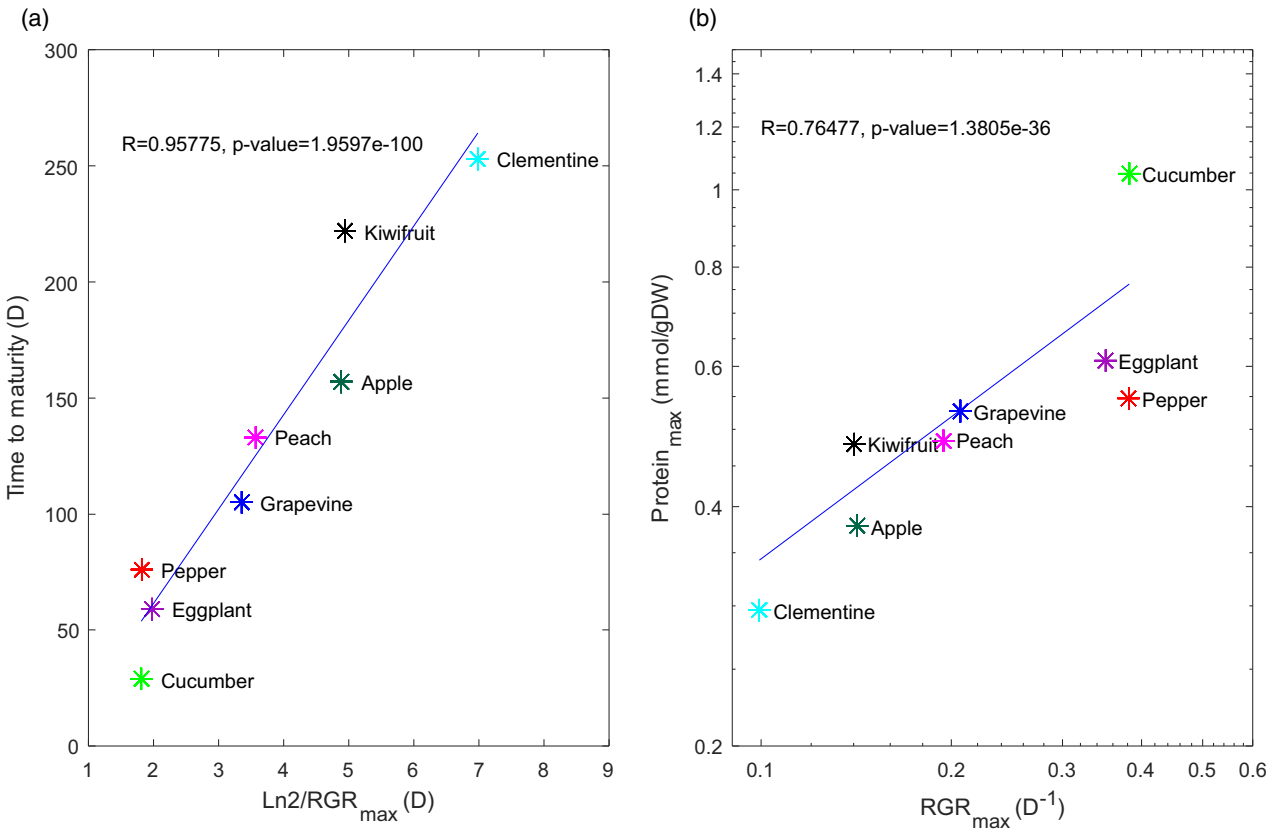

Figure 2. Relationship between the maximal relative growth rate (RGR_{max}) and (a) the time to maturity (days post anthesis, with RGR_{max} expressed as ln2-RGR_{max} ratio) and (b) the maximal protein content (mmol g^{-1} DW) in a panel of eight fruit species.

Table 1 Main fruit growth traits in a panel of eight fruit species

Fruit species	Time to maturity (DPA)	RGR_{max} (mmol g^{-1} DW D^{-1})	Time at RGR_{max} (DPA)	$[protein]_{max}$ (mmol g^{-1} DW)	Time at $[protein]_{max}$ (DPA)
Apple	157	0.1419	23	0.4167	2
Clementine	253	0.0993	37	0.3252	30
Cucumber	29	0.3827	7	1.1487	2
Eggplant	59	0.3508	5	0.7100	4
Grapevine	105	0.2067	0	0.7310	4
Kiwifruit	222	0.1403	1	0.5332	0
Peach	133	0.1944	32	0.6684	22
Pepper	76	0.3813	11	0.6605	5

DPA, days post anthesis; $[protein]_{max}$, maximal protein content; RGR_{max}, maximal relative growth rate.

A generic model to compare metabolic fluxes of eight fruit species

To make the comparison of metabolic fluxes between species possible, a model describing the central metabolism of a cell of the edible part of the fleshly fruits, and assuming homogeneous fleshly fruit tissue (Figure 3) was constructed based on previous work (Colombié et al., 2015, 2017). The role of this metabolic model was to import, store or transform extracellular nutrients, to ensure the growth of the organ but also to produce and regenerate antioxidants. The goal was to produce the main biomass components including major soluble sugars, starch, cell wall, organic acids, amino acids, proteins, lipids and phenolic compounds via the main metabolic pathways, sugar metabolism, glycolysis, pentose phosphate pathway, tricarboxylic acid (TCA) cycle, respiration and redox. For that, the previous models were implemented with (i) details of cell wall synthesis, which is the main carbon sink in the

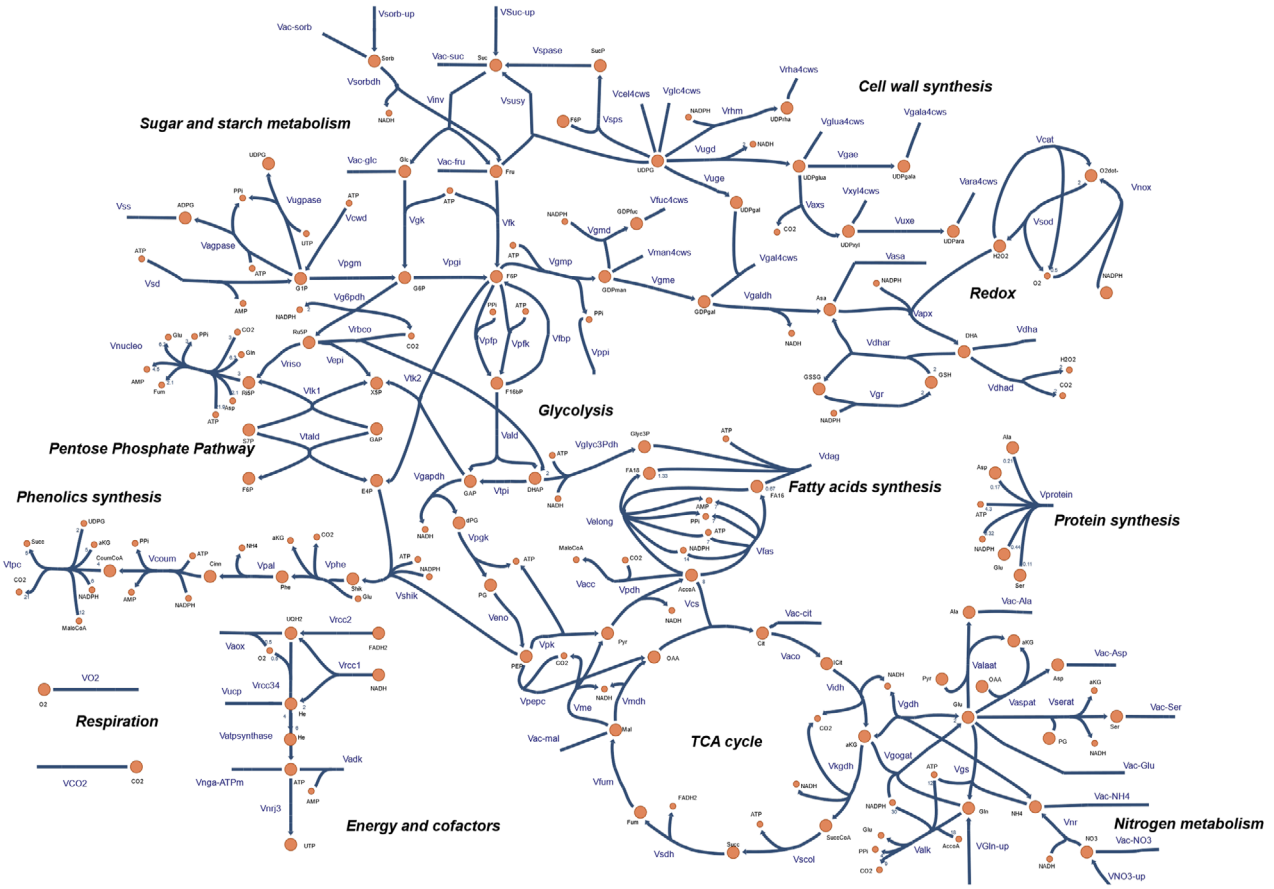

Figure 3. Scheme of the metabolic model with the main pathways (Escher Map Overview).

cell, i.e. synthesis of oligosides and two uronic acids (note that cell wall degradation is only one reaction as the sum of all negative fluxes); (ii) redox metabolism (ascorbate synthesis and ascorbate-glutathione cycling), which is essential during fruit development; (iii) secondary metabolism with the pathway towards total phenolics from their gallic acid precursor and (iv) mineral nitrogen metabolism involving nitrate, which can be stored or metabolised to ammonium and then to organic compounds. The sources of carbon and nitrogen, all being assumed to come from outside the fruit pericarp, mainly the phloem sap, have been simplified from the main metabolites common to at least two species. The carbon sources were sucrose, sorbitol and glutamine, while the nitrogen sources were glutamine and nitrate. All cofactors were defined as internal metabolites, which means that they were balanced, thus constraining the metabolic model not only through the carbon and nitrogen balance but also through the redox and energy status. The network of reactions schematised in Figure 3 is given as a list of the stoichiometric reactions (Table S1) and metabolites (Table S2) and provided as a Systems Biology Markup Language (*sbml*) file (Appendix S1).

A previous dataset for biomass composition of eight fruit species throughout their development (Roch et al., 2020) was complemented by measuring total phenolic compounds (TPC) and nitrate and ammonium inorganic ions (Table S3). By summing up the levels of these components expressed on dry weight basis, a high coverage of the biomass was explained for each stage of development and all fruit species (Table S4). For all species, at early stages, some biomass compounds were missing to cover the whole biomass such as non-crystalline cellulose, lignin or secondary metabolites. While it could lead to a potential bias of calculated fluxes at early stages, the fruit species comparison was still acceptable because all fruit species had the same behaviour. These interoperable data were then used to constrain the metabolic model, via the calculation of the corresponding external fluxes. For that, the data were first fitted in order to calculate the derivatives that were used as constraints for the metabolic fluxes (Table S5). Finally, the constraint-based model was solved to calculate metabolic fluxes throughout fruit development using the objective function of flux minimisation (minimisation of the sum of the squares of internal fluxes) in agreement with the principle of 'minimal effort'

(Holzhütter, 2004). To be able to perform multivariate analyses, flux data were generated at 30 developmental stages equally distributed throughout development. For each fruit species, time was normalised by the time to maturity (Table S6). Finally, the contrasted calculated fluxes, both external and internal, were analysed to bring out specific reactions and pathways supporting growth traits.

Flux distribution distinguishes developmental stages as well as fast- from slow-growing fruit

To compare the metabolism of the eight fruit species, a principal component analysis (PCA) was performed with all calculated fluxes (Table S7; Figure 4a). The first three principal components (PC) explained more than 70% of the total variance. PC1 separated young from ripe fruits, PC2 fast-growing from slow-growing fruits and PC3 growing fruits on the one hand from very young and ripening fruits on the other. The convergence of developmental trajectories along PC1 and PC2 resulted from the sharp decrease of most fluxes at the end of fruit development (Table S6). After this convergence, an increase following PC3 was still observed for the last four stages of development, in connection with a slight increase in several flows observed at the end of ripening in most species, involving mainly sucrose-phosphate synthase, alkaloids accumulation and cell wall degradation (Table S6). Although peach is a slow-growing fruit with a low RGR_{max} close to one of grapes (Figure 1b), its first stages of development along PC2 projected it on the side of fast-growing fruits. Indeed, the RGR of peach fruit peaked later and lasted longer than that of grapevine fruit, which peaked at the time of pollination, thus with less effect on overall fruit growth.

Hierarchical clustering analysis performed with all fluxes and RGR to produce a more detailed view of fluxes (Figure S4) revealed that most fluxes were distributed in three major clusters (Figure 4b). It allowed us to split the observation points into two main clusters, a cluster containing young stages of the four fastest-growing fruit species, cucumber, eggplant, pepper and peach (black cluster in Figure S4) and a cluster containing young stages of the four slowest-growing fruit species, apple, clementine, grapevine and kiwifruit (grey cluster in Figure S4). The behaviour of fluxes was very different between these two clusters. First, the green cluster named 'Growth', logically contained RGR, as well as fluxes that were clearly higher in the fast-growing fruits, i.e. most of the fluxes of accumulation of protein, amino acids, starch, lipids, cell wall, organic acids, hexoses, N-ions as well as the nitrogen uptake flux. Then, the blue cluster, named 'Glycolysis', mainly contained fluxes involved in sucrose metabolism (invertase and fructokinase), glycolysis (for instance triose-phosphate isomerase, glyceraldehyde-phosphate dehydrogenase, pyrophosphate-dependent phosphofructokinase, phosphoglycerate kinase, enolase and pyruvate kinase), pentose phosphate pathways (glucose-6-phosphate dehydrogenase, transaldolase and epimerase), sucrose uptake and ATP synthesis. Finally, the red cluster, named 'TCA&TPC' contained mostly fluxes involved in the TCA cycle (aconitase, fumarase, succinate dehydrogenase, isocitrate dehydrogenase and citrate synthase), reactions connected to the TCA cycle (glutamate dehydrogenase, pyruvate dehydrogenase, malic enzyme and phosphoenolpyruvate carboxylase), the whole synthesis pathway of phenolic compounds, respiration and the alternative energy pathway (maintenance, alternative oxidase and proton leakage). In the next paragraph we will focus on energy metabolism.

Slow-growing fruits use more energy to grow while fast-growing ones use more nitrogen

Respiration can be predicted from the constraint-based model as the CO_2 evolution (Sweetlove et al., 2013). Respiration rate was examined for the fruits throughout development as the sum of all fluxes of the reactions generating CO_2 in the model (Figure S5a). The high respiration rate during the first stages of development mainly for the fruits from trees lead to a high proportion of carbon uptake for apple, grapevine, peach and clementine, with about 30% of C-uptake (Figure S5b) converted into CO_2. Thus, long-lived fruits clearly released higher amounts of CO_2, especially during the young stages. Though we can notice a slight increase in CO_2 at the end of development for pepper and eggplant, the climacteric species, apple, peach and kiwifruit, did not show an increase in CO_2 release (Figure S5a).

Redox metabolism was connected to carbon metabolism and growth via the use of GDP-sugar for the synthesis of ascorbate and reactive oxygen species scavenging (H_2O_2, Figure 3). It is worth mentioning that for several species, it was necessary to add the degradation of oxidised ascorbate so that a solution could be found by modelling. The time-course of oxidised and reduced ascorbate fluxes (Figure S5e,f) showed that pepper and kiwifruit, and to a lesser extent grapevine, actively synthesised reduced ascorbate at the beginning of development while cucumber, eggplant and pepper also actively synthesised oxidised ascorbate, albeit at fluxes that were 10 times lower than the former. Interestingly, this result suggests that the higher oxidised ascorbate concentrations found in the fast-growing fruits (Roch et al., 2020) was the result of higher oxidation flux.

Carbon demand (sum of uptake fluxes from sucrose, sorbitol and glutamine expressed in mmol C g^{-1} DW day^{-1}) was compared throughout fruit development (Figure S5b). While its profiles roughly followed RGR (Figure 1c,d), maximal carbon demand was not significantly correlated with RGR_{max} (Figure 5a), confirming that carbon usage did not limit fruit growth rate (Roch et al., 2020).

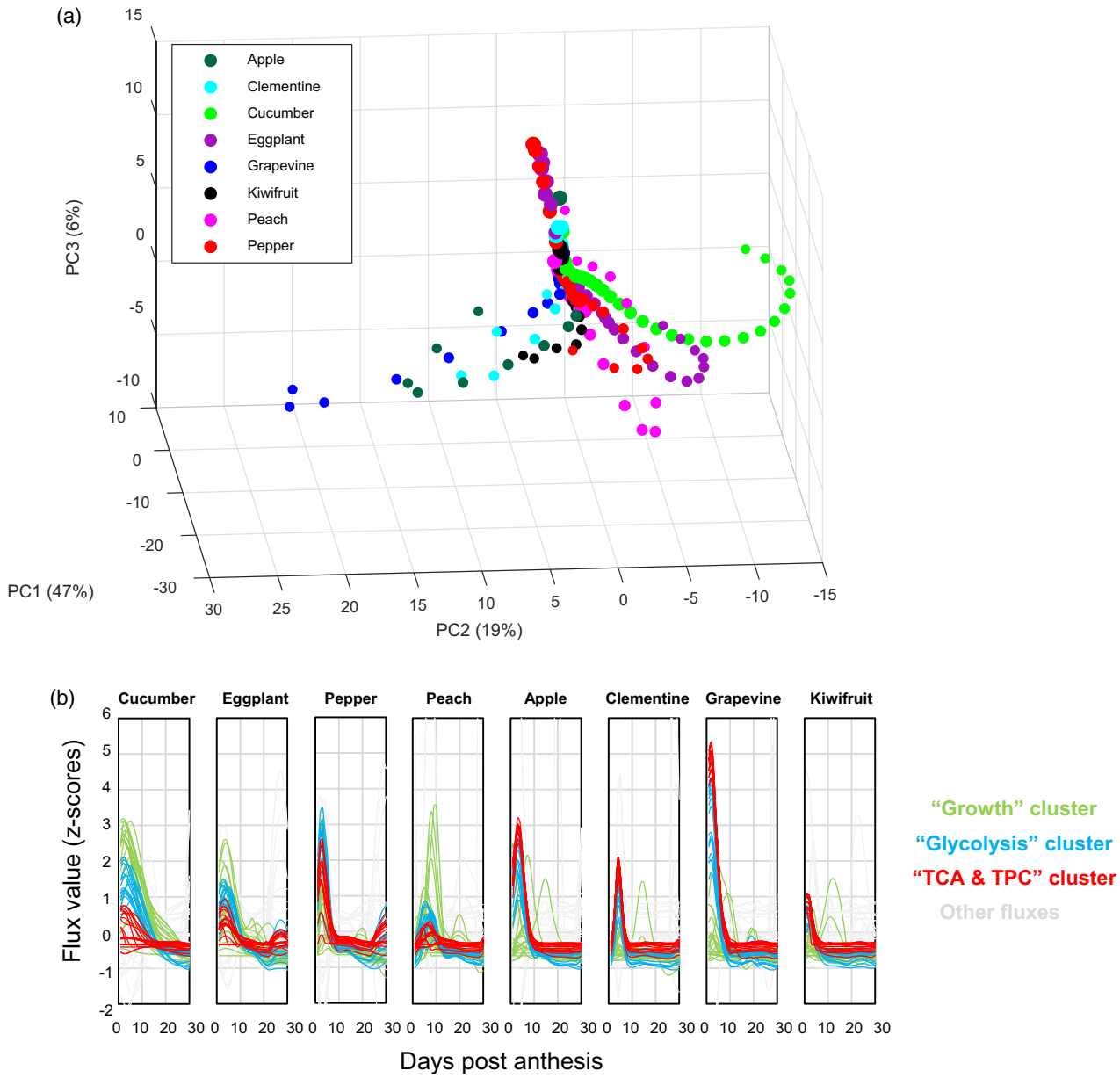

Figure 4. Fluxes (mmol g^{-1} DW D^{-1}) calculated at 30 stages of fruit development in a panel of eight fruit species separated by (a) 3D-principal component analysis (scores plot) and (b) hierarchical clustering analysis performed with Pearson coefficient as distance.

Conversely, nitrogen demand (sum of uptake fluxes from glutamine and nitrate expressed in mmol N g^{-1} DW D^{-1}) was linked with the growth profile (Figure S5c), and maximum N-uptake was significantly correlated with RGR_{max} (Figure 5b). Slow- and fast-growing fruits were clearly distinguished, with a maximum nitrate uptake lower than 0.2 mmol N g^{-1} DW D^{-1} for slow-growing fruits. As shown previously for RGR, peach displayed an intermediate N-uptake profile (Figure S5c), with a maximum slightly higher than that of grapevine but later and lasting longer, which brings this fruit species closer to fast-growing fruits. Thus, in the following section, special attention was paid to nitrogen metabolism.

Nitrogen assimilation as a booster of fruit growth rate

As mentioned above, the main biomass component discriminating the two major fruit types were three nitrogenous compounds: proteins, free amino acids and inorganic nitrogen (nitrate and ammonium) (Figure S2a,b,e). It is striking that cucumber, pepper, and eggplant presented relatively high nitrate contents. Fast-growing fruits had higher nitrogen content at anthesis and young stages,

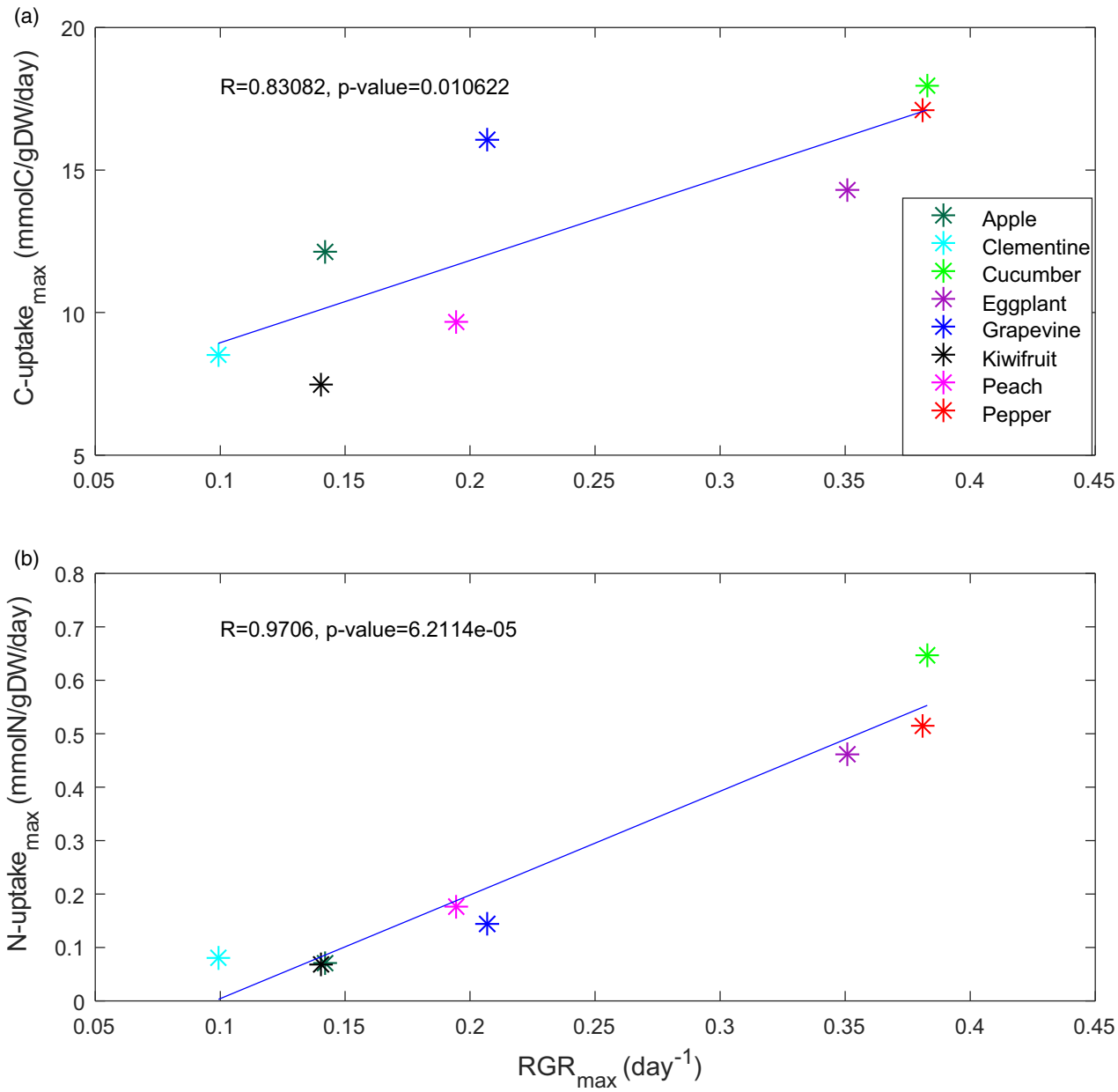

Figure 5. Linear correlation between RGR_{max} and the maximal (a) carbon uptake and (b) nitrogen uptake flux ($C\text{-}uptake_{max}$ and $N\text{-}uptake_{max}$, respectively) in a panel of eight fruit species.

which led to higher nitrogen demand and resulted in higher nitrogen uptake rates (Figure S5c). In fruit, nitrogen is usually considered to be supplied in the form of amino acids. The generic model developed here assumed glutamine as the supply form (Figure S6a). It is, however, known that other amino acids can be supplied, for example, citrulline in cucumber (Ohyama, 2010) but with a fruit content about 10 times lower (Corleto et al., 2019), citrulline was not considered in the model, and glutamine was assumed to be the main amino acid imported from phloem sap. To account for the nitrate content, and also allow for significant nitrate reductase (NR) activity for faster-growing fruits (e.g., cucumbers and peppers) for more than the first half of development, the model surprisingly suggested high uptake of mineral nitrogen (nitrate, Figure S6c). To validate this result, NR activity measurements were performed for all fruit species, at least for the first stages and for all stages when activity was detected (Table S8; Figure 6a). Interestingly after flux conversion from DW to FW using the calculated ratio, a significant and positive correlation was obtained between NR activity and estimated NR flux throughout cucumber fruit development,

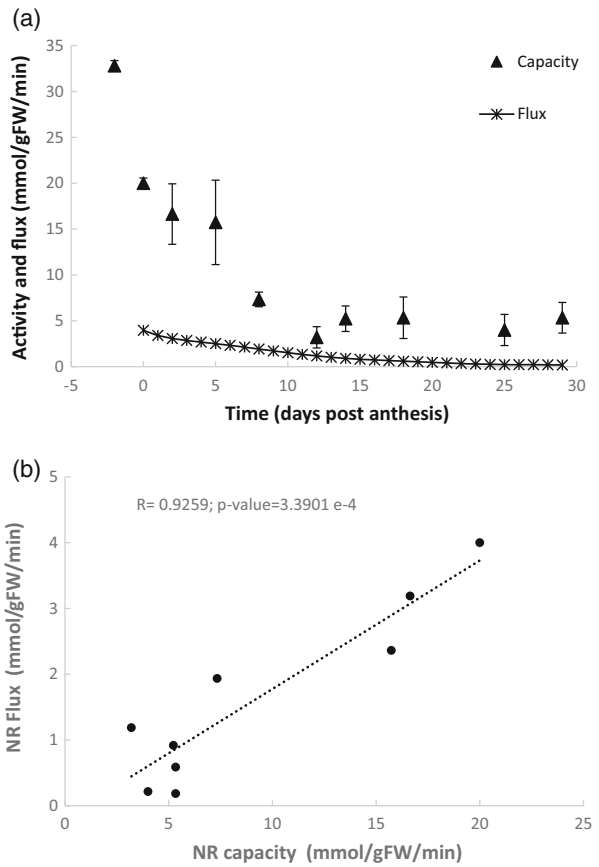

Figure 6. (a) Time-course of the calculated flux of nitrate reductase (NR, mmol g^{-1} FW min^{-1}, 30 stars and line) and the NR enzyme capacity measured at 10 stages (triangles) of cucumber fruit development with (b) the linear correlation between the two, flux and enzyme capacity.

with flux values reaching around 20% of the maximal activity (Figure 6b) in all development stages. Similar results have also been reported for *Brassica napus* embryos (Junker et al., 2007), with enzyme activities present in a large surplus relative to their requirements for the observed in vivo fluxes. The model also suggested nitrate assimilation via NR during a short part of fruit growth for eggplant and peach (Figure S6c). In agreement with the model calculation, a low NR activity was found in peach at the first sampled stage of development (22 days after anthesis [DPA], Table S8). To balance nitrogen at the end of development, an output flux was added in the model.

Rearrangement of nitrogen metabolism leads to the accumulation of alkaloids in ripening pepper and eggplant

Another unexpected result was that for several fruit species, especially pepper and eggplant (two Solanaceae) the accumulation of N-containing compounds was required at ripening in conjunction with cell wall degradation (Figure S7). We identified alkaloids as the probable nitrogen sink in Solanaceae (Mennella et al., 2012). To validate this result, the alkaloid amount was estimated from the flux (*Valk*), as its accumulation each day. The final concentration of alkaloids was 4 and 6 mmol per fruit for pepper and eggplant, respectively, at the last stage of development. These values correspond to, respectively, 22 and 7 μmol g^{-1} FW considering the final fruit weight of both pepper and eggplant (184 and 839 gFW $fruit^{-1}$, respectively). From a modelling point of view this reaction was required to balance nitrogen, more precisely to clear out nitrogen excess at the end of development. In Solanaceae fruit, main alkaloids include α-tomatine, solanine and solasonine (Ohyama et al., 2013). To verify these results with experimental data, we searched for alkaloid contents in the literature. For instance, in eggplant fruit, solasonine reaches 0.2 mg g^{-1} FW (Bagheri et al., 2017) and the content of solamargine and solanine, two major alkaloids, can reach 5 mg g^{-1} FW (Friedman, 2015; Friedman & Levin, 1995). Our estimation of 22 μmol g^{-1} FW corresponds to 19 mg g^{-1} FW. Similarly, in pepper fruit, capsaicinoid compounds, responsible for the pungency with capsaicin and dihydrocapsaicin constituting 90% of these compounds (Hamed et al., 2019) can reach 10 μmol g^{-1} DW (Barbero et al., 2016). Although slightly higher than the reported measured values, our model estimations were of the same order of magnitude. To go deeper in the analysis, in the next section, special attention was paid to decipher the main pathways involved during fruit growth.

Rapid growth mobilises glycolysis rather than the tricarboxylic acid cycle

Another striking trend highlighted by the flux clustering analysis (Figure S4) was found for fluxes of the Glycolysis and TCA&TPC clusters, especially in the young stages. In slow-growing fruits, fluxes of the TCA&TPC cluster were always higher than those of the Glycolysis cluster (Figure 4b). We observed a complete metabolic shift between fast- and slow-growing fruits, with the fluxes of the Growth cluster exceeding those of the Glycolysis cluster exceeding those of the TCA&TPC cluster in the former fruit type and the reverse in the latter. The fact that fluxes corresponding to the construction of primary structures (protein, cell wall and accumulation of osmolytes) were found in the Growth cluster while those located upstream of phenylpropanoid metabolism (i.e., V_{phe}, V_{pal}, V_{shik} and V_{coum}) in the TCA&TPC cluster suggests the existence of an energy-based trade-off between growth and accumulation of specialised metabolites.

To explore more conceptually the role of the biomass compounds, the next step was to build virtual fruits with a wide range of biomass composition, to calculate the metabolic fluxes throughout their development and then to analyse the flux distribution of these virtual fruits.

Virtual fruits decipher the influence of biomass composition on metabolic pathways

The PCA of the metabolic fluxes made it possible to identify the fluxes that contribute the most to the construction of the PCs but not to identify the biomass components whose synthesis and/or accumulation would be responsible. For this, virtual fruits were designed to evaluate the effect of the 12 major biomass components on metabolic fluxes and pathways. Thus, to build virtual fruits, a common and unique fruit growth pattern was used, defined as the median fruit growth rate of the eight species throughout fruit development (Figure S8a). Then, the fluxes towards the 12 major biomass components, namely cell wall synthesis, redox, fatty acids, cell wall degradation, free amino acids, proteins, organic acids, soluble sugars, starch, nucleic acids, total phenolics and accumulated nitrogen compounds, were set up at a high (calculated as the mean of the eight fluxes of fruit species plus 2 × Standard Deviation, in mmol g^{-1} DW D^{-1}) or low (10^{-3} mmol g^{-1} DW D^{-1} throughout fruit development) level (Figures S8b,ae and S9). A fractional experimental plan was used to perform 128 virtual experiments with combinations of these 12 virtual profiles set up at high or low levels (Table S9). Then, 32 virtual experiments were removed because the corresponding mean biomass accumulated was too low (less than 200 mg g^{-1} DW) to be physiologically relevant, and 96 experiments were kept for further analysis (Figure S10). For these 96 virtual fruits, the effect of each of the 12 major biomass component factors was evaluated on two overall variables calculated throughout fruit development, i.e. the final cumulative fluxes of carbon uptake (C-uptake) and nitrogen uptake (N-uptake) (Figure S11). Soluble sugars (i.e. glucose, fructose and sucrose) and cell wall components (10 monosaccharides and uronic acids) were the most influential factors regarding final cumulative carbon uptake (Figure S11a). Regarding nitrogen uptake, soluble sugars and cell wall components were important factors, but free amino acids and total phenolics also had a high effect (Figure S11b). To go further and to visualise the effect of the 12 major biomass components on metabolic fluxes, the 96 virtual fruits were projected on the 3D-scores plot of the PCA performed (Figure 4a) with the fluxes of the eight real fruits (Figure S12). For most of the biomass components, the separation of fluxes of virtual experiments was distributed along the three axes, as illustrated for free amino acids, sugars, lipids and cell wall degradation (Figure S12a–f). A particularly clear separation between virtual fruits was obtained for cell wall synthesis (Figure S12e) and total phenolics levels (Figure S12f) along PC2 and PC1, respectively. Among the virtual fruits, only those with high cell wall synthesis fluxes and low phenolic compounds synthesis fluxes clustered with the fast-growing real fruits. Conversely, only virtual fruits with high phenolic compounds synthesis fluxes and low cell wall synthesis fluxes clustered with the slow-growing real fruits (Figure 7). The contribution of phenolics appeared here because the fruit growth, similar for all virtual fruits, did not impact the metabolic fluxes. In other words, virtual fruits with median fruit size and similar time to maturity, made it possible to explain the effect of each biomass compound on metabolic fluxes. Indeed, the contribution of phenolics especially for slow-growing fruits was erased in the small fruits and could not be shown with real fruits. This result suggests a trade-off between growth and synthesis of specialised compounds involved in defence. Indeed, the clustering of fluxes of these virtual fruits clearly showed that high cell wall and low phenolics were responsible of high fluxes in both clusters, Growth and Glycolysis clusters (Figure S13a). Conversely the TCA&TPC cluster was associated to high phenolics and low cell wall (Figure S13b). The metabolic trade-off was confirmed by calculating the correlation coefficients between 119 fluxes and RGR values extracted at the fourth stage of development among 30 in the panel of the eight fruit species (Table S10; Figure S14). Interestingly, most of negative values of correlation coefficients were obtained between reactions of Growth cluster (green) and TCA&TPC cluster (red) supporting that constraint-based metabolic modelling allowed to find trade-offs as described in Hashemi et al. (2023).

DISCUSSION

The purpose of this study was to analyse to what extent fruit growth rate depends on carbon and nitrogen metabolism. The use of a panel of eight species grown under optimal production conditions regarding fertilisation and light revealed a close relationship between RGR and the duration of fruit development. The comparison of metabolic fluxes, calculated throughout fruit development using time-series of unlabelled metabolite data and constraint-based modelling, then highlighted the key role played by nitrogen metabolism and the existence of a trade-off between cell wall synthesis and accumulation of specialised metabolites. Thus, all fruit species have similar carbon and energy requirements to reach maturity, whether it is fruit from trees which grow slowly or fruits from herbaceous which grow faster. Rapid fruit growth required rapid construction with more available nitrogenous resources, especially proteins, to ensure a high RGR.

Note that in the present study, we did not consider the influence of the environment (e.g. temperature humidity, radiation). Actually, for each species we calculated the GDD and results were unchanged when time was expressed as GDD, absolute or normalised by the time to maturity (Figure S1). This observation is in agreement with (Zhu et al., 2018) who studied the spatiotemporal variation

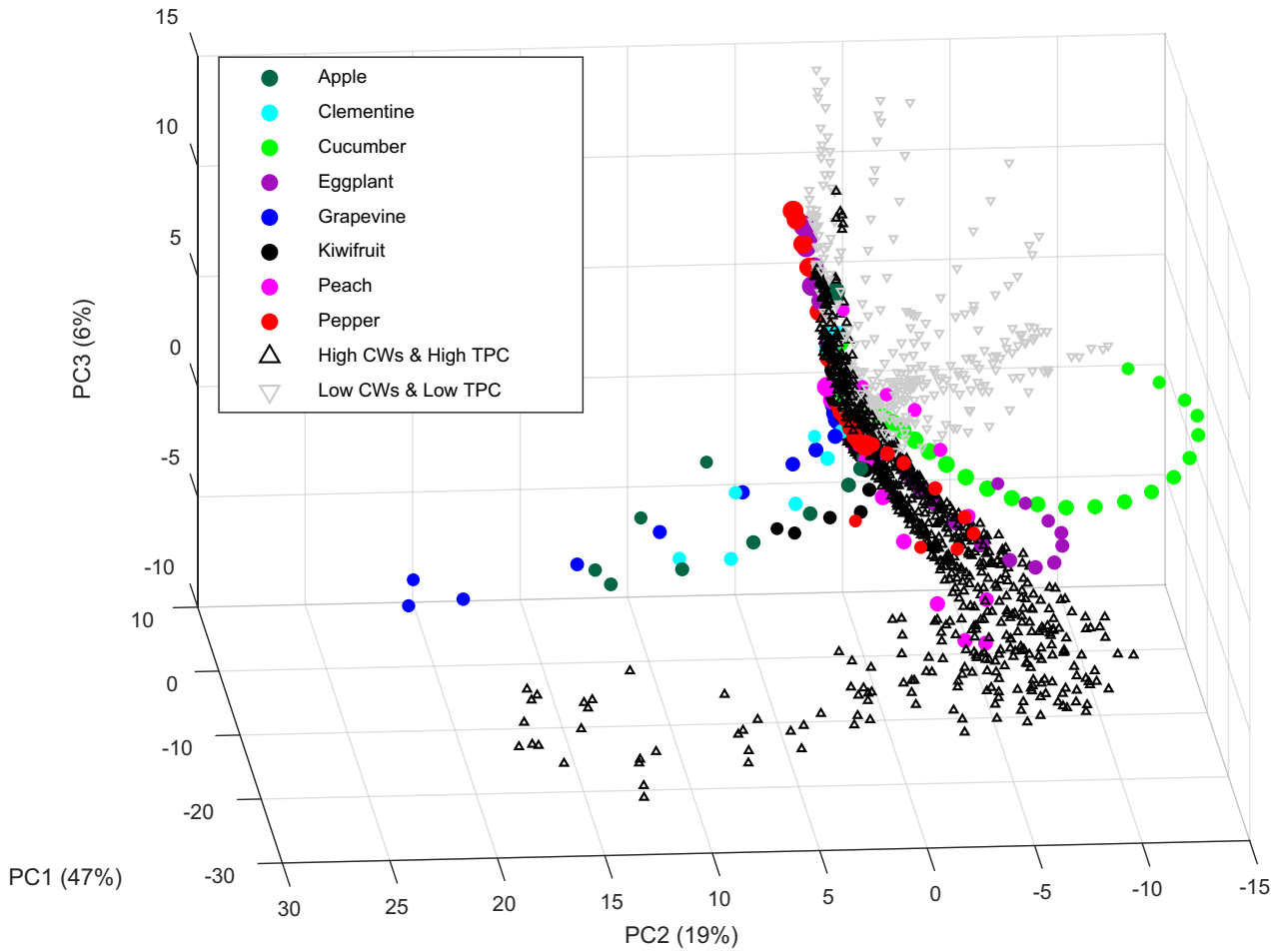

Figure 7. 3D-principal component analysis performed with fluxes calculated in a panel of eight fruit species (Figure 4a) with added projected fluxes calculated from selected virtual experiments with cell walls (CWs) high and total phenolic compounds (TPC) low (▲) and conversely CWs low and TPC high (▼).

in the phenology of two herbaceous species and associated climatic driving factors on the Tibetan Plateau during 2000–2012.

The link between growth rate and development time is a potentially useful allometric relationship

The concept of allometry was initially proposed to make the link between organ sizes through the use of mathematical models (Huxley & Teissier, 1936). It has since diversified as other notions have been associated with the size of organs or individuals, within species or between species, such as metabolic activity (Davison, 1958). The significant relationship found here relates the maximal RGR that reflects metabolic activity to the duration of the development of an organ. The use of literature data for eight other fleshly fruit species indicates that this relationship can be generalised (Figure S14). It will be interesting to check whether it exists for other organs such as seeds (Gómez-Fernández & Milla, 2022) or even taxonomic groups other than higher plants as previously done with several taxa (Arendt, 1997). This ontogenetic relationship is not trivial because it implies that the developmental trajectory of the fruit is decided – at least for a large part – from the start of growth. In other words, there would be no stationary state, during which the functions of the organ would be maintained indefinitely thanks to housekeeping functions.

A major point is that the maximum total protein concentration in fruit flesh was strongly correlated with RGR_{max}. As previously suggested (Roch et al., 2020), fruit RGR would depend on the amount of catalysts, hence proteins, under the hypothesis that growth is limited by the capacity for protein synthesis (Elser et al., 2000). The results obtained here suggest that the way in which protein metabolism functions at the time of pollination or just after also conditions the duration of development. It will therefore be important to study protein turnover in detail, using labelling and/or modelling approaches (Belouah et al., 2019; Li et al., 2017), in order to identify what conditions protein concentration and therefore limits growth rate. We speculate that such a study would greatly benefit from cross-species

comparison. Although such allometric approach remains rare, it is very promising. For example, when questioning phenotypic differences between organisms with three genome-wide datasets of human-mouse orthologs arising from a variety of sources in protein divergence Morata et al. (2013) identified a relationship between protein divergence and isoform multiplicity co-occurrence and explained its origin in terms of a simple gene-level property. The implications of these findings could be used to analyse the molecular basis of differences between species, as they provide a plausible explanation regarding the balance between function and cost of synthesis constraints.

The duration of the development of certain fruits, in particular the fruits of many woody plants in which it can exceed 200 days, can be seen as an important trait. Indeed, the longer it takes for a fruit to grow and ripen, the higher the probability it will be impacted, whether by biotic stress or by extreme climatic events. For a breeder, it will probably be tedious to screen genetic diversity for the duration of development, but it was done for peach species in order to cover the entire production season, thanks to early varieties with short development times (Byrne et al., 2012). On the other hand, it will be interesting to consider the protein concentration of the ovary or the very young fruit, which is relatively easy to measure, as a proxy for the duration of development.

Modelling of metabolic fluxes suggests that nitrogen metabolism controls growth rate

In line with the major role played by protein metabolism, fluxes involving nitrogen compounds, from amino acids and – in some cases – nitrate to total protein, have been found to be strongly correlated with RGR during early stages of fruit development while carbon import and utilisation appeared uncorrelated. This is in agreement with Poorter and Bergkotte (1992) who showed that fast-growing species accumulated more organic N-compounds and with Dai et al. (2016) who showed that carbon utilisation for synthesis of non-soluble sugar compounds was conserved among grape, tomato and peach.

Unexpected results obtained here suggest that NR, which is considered as the most rate-limiting enzyme for nitrate assimilation (Chamizo-Ampudia et al., 2017), may contribute to growth rate in fast-growing fruits, especially cucumber. There are very few studies that have looked for this enzyme in fruits. In apple fruit, no NR activity was reported for two cultivars (Zhang et al., 2011), although a low content of nitrate was found during fruit growth and development. In grape berries (Cabernet Sauvignon), a low activity of NR was measured and modulated such as amino acid levels and protein content under mixed nitrogen treatments, impacting both nitrogen and sucrose metabolism (Yin et al., 2020). In tomato fruit (Teitel et al., 1986), NR activity was found to be induced by nitrate supply at levels within the range of activities found here (1–10 mmol g^{-1} FW min^{-1}). NR activity was also found in papaw (Menary & Jones, 1972) and cashew (Subbaiah & Balasimha, 1983) at values within the same range. Nitrogen metabolism of pepper fruits, including NR activity, was influenced by both various light conditions and different nitrogen forms applied with fertilisers (Kołton et al., 2012). These studies showed that nitrate assimilation contributed to a few % of fruit organic nitrogen content. It may therefore seem interesting to increase nitrogen fertilisation to boost fruit growth. However, it is likely that N-fertilisation is already luxurious in usual fruit production (Carranca et al., 2018), and the excessive addition of nitrogen fertiliser is considered detrimental for fruit, impacting quality and even development duration (Lang et al., 2018). It might be interesting to test the effect of nitrogen fertilisation during early fruit development and even flowering, to see if it boosts growth. However, such a practice would be difficult to implement, especially because nitrogen is known in agriculture to delay flowering. In fact, most of the nitrogen taken up by the fruit results from the translocation of amino acids from other plant parts. The supply of nitrogen to the fruit therefore results from a set of mechanisms that are still relatively poorly understood. Here are a few examples to illustrate this complexity. In cucumber, high potassium fertilisation was found to exert a positive effect on the uptake and assimilation of nitrate in leaves, as well as an improved translocation of amino acids towards the fruit (Ruiz & Romero, 2002). In eggplant, more efficient remobilisation of N from leaves to fruits was proposed as a strategy to improve nitrogen use efficiency, a trait that will become increasingly important in sustainable agriculture (Mauceri et al., 2020). In pepper, an appropriate ammonium to nitrate ratio of 1/3 in nitrogen application was found to stimulate root development and enhance yield and fruit quality (Zhang et al., 2019). More generally, a better understanding of nutrient requirements with improved rates and timings of N-fertilisation is needed for an efficient yield of high-quality fruits (Carranca et al., 2018).

In the present study, peach was systematically closer to herbaceous fruit species than tree and vine species, especially during the early stages of development. This surprising and unexpected behaviour of peach could be linked to endoreduplication in flesh cells, as the four fruits showing rapid growth (three herbaceous fruit species and peach) are known to display more than four endocycles (Chevalier et al., 2011), whereas no endocycle was reported for the other four species. It was suggested that endoreduplication may have an impact on global nitrogen metabolism in tomato-developing fruit (Mathieu-Rivet et al., 2010). Thus, in fruit of tomato plants overexpressing the Anaphase Promoting Complex activator CCS52A, endoreduplication and fruit growth were initially delayed. Recently,

Moreno et al. (2020) reported that nitrate regulates shoot growth by modulating cell size and endoreplication through the LGO gene as a regulatory factor influencing ploidy in *A. thaliana*. Interestingly, using a peach genotype with a slow ripening (SR) phenotype, compared to the WT Fantasia (FAN) nectarine, (Farinati et al., 2021) showed a progressive increase in ploidy level in the late phases of FAN fruit development but not in SR fruit. In addition, during fruit growth, the impaired expression of genes controlling cell cycle and endocycle resulted in the small final size of SR fruit. These studies suggest a positive relationship between the involvement of nitrogen in nucleic acids (DNA) with ploidy level and fruit growth and ripening.

Afterwards, it would also be interesting to add in the model a more detailed description of redox metabolism connected to primary metabolism involving nitric oxide and other reactive nitrogen species as important signalling molecules involved in a range of physiological changes (Hancock, 2019) during fruit development and ripening (Zhang et al., 2011). For instance, photosynthesis at early and green stages could drive NR activity by an excess of redox available similar to what was shown for fatty acid synthesis in green oilseeds (Ruuska et al., 2004). To capture the complex and highly regulated pathways, a detailed description of interconnected biochemical reactions with an accurate genome-scale metabolic network is needed, with the combination of specific methods such as FlexFlux (Marmiesse et al., 2015), to analyse both metabolic and regulatory networks. To encompass the dynamics of fruit development, the model could also evolve towards a mechanistic representation of fruit ontogenetic processes into physiological and ecosystem models such as the work performed to model changes in leaf-level photosynthetic capacity as a function of leaf biochemical constraints (costs of synthesis and defence), nitrogen availability and light (Detto & Xu, 2020).

The trade-off between cell wall and specialised metabolites is a trade-off between growth and defence

The comparison of flux distributions highlighted a trade-off between growth and accumulation of defence-related compounds (see the recent review He et al., 2022). Thus, in fast-growing fruits, carbon and nitrogen were more rapidly metabolised to cell wall and protein synthesis. Rapid growth imposes high cell wall synthesis fluxes, as this is essential for the survival of plant cells (Beauvoit et al., 2018). According to the network described in Figure 3, cell wall synthesis uses UDP-glucose, itself synthesised from sucrose via the reaction catalysed by sucrose synthase or via the reaction catalysed by UDP-glucose pyrophosphorylase, which consumes one glucose-1P, i.e. less than one ATP equivalent required per unit of cell wall sugar. It, therefore, seems logical that glycolysis would be used more as it leads to less complete oxidation of sugars for less ATP produced. Conversely, fluxes towards the synthesis of total phenolics were much higher than in fast-growing fruits, especially during early growth. The accumulation of phenolic compounds (Table S3), which can be seen as a defence mechanism linked to the increase in the duration of exposure to various stresses, consumes significantly more energy per unit of phenolic compounds. The synthesis of phenolic compounds is also closely associated with the TCA cycle since it consumes 2-oxoglutarate and co-produces succinate. It is actually striking that fluxes in the TCA cycle appeared mainly driven by the synthesis of phenolic compounds, and not by other processes requiring ATP or carbon skeletons such as protein synthesis.

Such trade-off appears in agreement with Bekaert et al. (2012), who used flux balance analysis to estimate fluxes with or without glucosinolates synthesis in *A. thaliana* and estimated an increase of at least 15% of photosynthetic requirements to support the metabolic costs for glucosinolate production. Paradoxically, although our results suggest that fast growth (accumulation of osmolytes and synthesis of cell wall) and rapid accumulation of defence compounds cannot occur simultaneously, carbon did not seem to be a limiting factor for the RGR of the fruit (Figure 5). In fact, the trade-off between growth and defence probably is universal and particularly important for plants that must constantly adjust the use of resources between growth, which accelerates the acquisition of further resources, and defence against the many stresses to which they are subjected (Cope et al., 2021). In their review Karasov et al. (2017) investigated how defence costs are generated and how they could be mitigated. Most of the well-characterised trade-offs between growth and defence have been found to stem more from antagonistic crosstalks between hormones than from metabolic limitation. Thus, salicylic acid and jasmonic acid, which are involved in defence, counteract the action of growth-promoting hormones such as gibberellins and auxin. It is, therefore, conceivable that such crosstalk is at work in fruits, in particular at the start of growth, which is characterised by high levels of gibberellins and auxins (Beauvoit et al., 2018; Fenn & Giovannoni, 2021). It will be interesting to check whether this trade-off can be generalised, for example, by extending the approach taken here to a greater number of fruit species. It will also be interesting to conduct a comparative study of the dynamics of hormones and transcriptomes during fruit development of multiple species, to validate the hypothesis of the existence of an antagonistic crosstalk between stress and growth hormones during fruit growth.

EXPERIMENTAL PROCEDURE

Fruit material and growth conditions

This study was conducted with eight fleshly fruit species, apple (*Malus* × *domestica* Borkh. cv Golden), cucumber (*Cucumis sativa*

L. cv Aljona), clementine (*Citrus reticulata* × *Citrus sinensis* cv SRA 63) eggplant (*Solanum melongena* L. cv Monarca RZ), grapevine (*Vitis vinifera* L. cv Cabernet Sauvignon), kiwifruit (*Actinidia deliciosa* Chev. cv Hayward), peach (*Prunus persica* L. cv Nectarlove) and pepper (*Capsicum annuum* L. cv Gonto Clause) whose growth conditions were described before (Cakpo et al., 2020; Roch et al., 2020). Experiments were performed under optimal conditions in France, in orchards for peach, apple, kiwifruit and clementine, in a plastic tunnel for pepper, or in a greenhouse for grape, cucumber and eggplant.

During fruit development, at least 10 sampling dates were monitored. Samples were collected from anthesis or early growth stages to maturity. For each species, the developmental stage was identified as the number of DPA. To compare fruit development, time was expressed as GDD, related to the accumulation of average daily temperatures:

$$\mathrm{GDD} = \max\left(T_{\mathrm{average}} - T_{\mathrm{base}}, 0\right) \quad (1)$$

with T_{average} the average of daily temperature and T_{base} the base temperature, considered as the minimum development threshold temperature. T_{base} was set to 4°C for apple and grapevine, 7°C for peach (Marra et al., 2002), 8°C for Kiwifruit, 10°C for pepper, eggplant, and clementine, and 15°C for cucumber (Hoyos García et al., 2012). During sample preparation, physical measurements (fresh mass, height and diameters) were taken on each fruit to estimate the growth accurately. The five biological replicates of pericarp samples were then deep-frozen in liquid nitrogen and stored at −80°C before cryogrinding, lyophilisation and biochemical analyses. Lyophilisation allowed measurement of the dry matter content. Sample dry matter was calculated from the dry matter content and measured fresh mass.

Growth data were added from published studies for eight other fruit species: atemoya (https://www.ttdares.gov.tw/en/theme_data.php?theme=what_we_do&sub_theme=achievements&id=6178), avocado (Liu et al., 1999), blood orange (Chen et al., 2022), mango (Tandon & Kalra, 1983), pear (Oikawa et al., 2015), strawberry (Cakpo et al., 2020), sweet cherry (Gibeaut et al., 2017), and tomato (Biais et al., 2014).

Quantification of biomass compounds and accumulated metabolites

Most of metabolites and biomass compounds were reported in Roch et al. (2020). To complement the description of fruit biomass, total phenolic compounds, total DNA and nitrate and ammonium were measured in the present.

For TPC, frozen aliquots of 100 mg FW were mixed with 1 ml of aqueous 60% methanol and 1% acetic acid (v/v/v) and extracted for 30 min using an ultrasonic bath at 4°C. After 10 min centrifugation at 4000 ***g***, supernatants were collected, and the extraction was repeated. Then, technical duplicates of 0.2 ml of extract or standard solution for calibration (50, 100, 150 or 200 mg L^{-1} gallic acid in 60% aqueous methanol and 1% acetic acid were mixed with 1 ml of 0.2 N Folin–Ciocalteu reagent and 0.8 ml of 75 g L^{-1} Na_2CO_3). After 30 min incubation at room temperature and in the dark, absorbance was measured at 760 nm against a blank (Cary Bio 1 Spectrophotometer, Varian, Australia).

Total DNA content was measured using the deoxyribose-specific diphenylamine reaction according to the method described in Colombié et al. (2015).

Ammonium and nitrate were extracted and assayed according to Carillo et al. (2019) with few modifications. Fruits powdered dried tissues (50 mg) were suspended in 5 ml of Milli-Q grade water (Milli-Q PLUS; Millipore, Burlington, MA, USA), and then subjected to three freeze–thaw cycles. The clear supernatants obtained after centrifugation were assayed by ion-exchange chromatography using a DX500 apparatus and columns (Dionex, Sunnyvale, CA, USA). In particular, an IONPAC-ATC1 anion trap column, an IONPAC-AG11 guard column and an analytical IONPAC-AS11 4-mm column, fitted with an ASRSII 4-mm suppressor for nitrate, and an IONPAC-CTC cation trap column, an IONPAC-CG12A guard column (Dionex) and an analytical IONPAC-CS12A 4-mm column, fitted with a CSRS 4-mm suppressor for ammonium, coupled to a CD20 conductivity detector were used. The extracts (20 µl) were injected onto the columns and eluted at a flow rate of 2 ml min^{-1} in isocratic mode for 15 min. The solvent used were sodium hydroxide 5 mM for anions and methanesulphonic acid 20 mM for cations, respectively. Nitrate and ammonium concentrations were determined against standard curves in the range 0.05–0.5 mM and expressed as µmol g^{-1} DW.

Quantification of NR activity

Nitrate reductase activity was extracted and measured on fresh frozen powder under substrate-saturating conditions as described in Gibon et al. (2004).

Stoichiometric model

The model is given in Tables S1 and S2 for the list of reactions and metabolites and Appendix S1 for the model in *sbml* format.

Resolution of the model and flux calculations

Steady-state

The model of the metabolic network describes the cell metabolism through a set of n reactions involving m metabolites of which m_{int} were internal metabolites. At steady-state, the mass balance equation is expressed by

$$\frac{dX_{\mathrm{int}}}{dt} = NV = 0 \quad (2)$$

With X_{int} the vector of m_{int} internal metabolites, V the flux vector composed by the rates of n reactions of the network, and N the stoichiometry matrix. To solve the system and reduce the solution space, a lower and an upper bound constrained each flux.

Constraints limiting the flux space

First, thermodynamic properties were used to constrain fluxes from reversibility to irreversibility. Thus, among the 119 internal reactions of the metabolic network, 44 were irreversible, which meant that their lower bounds were set to zero.

The most important constraints required to set up the system were the external fluxes, also called exchange fluxes. The mass balance of accumulated metabolites and biomass components covered the dry biomass. The corresponding external fluxes (accumulation rates towards accumulated metabolites and biomass components and glucose uptake rate) were calculated from experimental data (Table S5). For all biomass compounds and accumulated metabolites (expressed in mmol/fruit), the best polynomial fitting on experimental data was searched (criteria r^2 maximum). The corresponding fluxes (accumulation and/or degradation) were then calculated by calculating the first derivative of the fitted functions. These fluxes were used as lower and upper bounds to constraint the resolution of the model. In the

case of reversible enzymes, the lower bound was negative. Growth and DW-to-FW ratio were also fitted in order to further convert fluxes from a fruit-basis to a gram-basis. In the case of amino acids, the total concentration of amino acids was split into four groups defined by their precursors (Table S5). Regressions of the experimental data were performed using the R shiny interface EasyReg (https://sprigent.shinyapps.io/regshiny/) using basic and *nlstools* R packages.

Objective function

Flux minimisation, more exactly the minimisation of the sum of the squares of all internal fluxes, which leads to a unique solution (minimal consumption of the available resources; Holzhütter, 2004), was used as the objective function to solve the system and calculate fluxes each day of development.

Software

Stoichiometric model and mathematical problems were implemented using MATLAB (Mathworks R2018, Natick, MA, USA) and the optimisation toolbox, solver *quadprod* with interior-point-convex algorithm for the minimisation.

Statistical analyses

Hierarchical clustering analysis of flux data with RGR used to select three clusters was performed with MultiExperiment Viewer (RRID:SCR_001915, MeV4.9.0). PCA of flux data of real fruits was performed using BioStatFlow web tool (http://biostatflow.org; Jacob et al., 2020) after mean-centring and unit-variance scaling. The data comprised 119 flux variables for the 240 samples (eight fruit species at 30 stages). The PCA loading values were then used to project the 96 virtual fruits at 30 stages on the PCA scores plot, using the 119 calculated flux data for the 2880 virtual samples (96 virtual experiments at 30 stages). The scores were plotted in 3D using MATLAB *scatter3* (Mathworks R2018). Relationships between variables were studied using Pearson correlations, and their p-values calculated using MATLAB.

Hierarchical clustering of flux and RGR *z*-scores (by rows) was performed using MultiExperiment Viewer (RRID:SCR_001915, version 4.9.0) with Pearson correlation as distance and average linkage.

ACKNOWLEDGEMENTS

We thank Léa Roch for fruit cultures, harvesting and previous analyses, the Bordeaux Metabolome Platform (https://doi.org/10.15454/1.5572412770331912E12) for providing data, Daniel Jacob for managing data, Gilles Vercambre for thermal time calculations, and Jean-Pierre Mazat for his critical reading. This work was supported by FRIMOUSS (ANR-15-CE20-0009-01), MetaboHUB (ANR-11-INBS-0010), PHENOME (ANR-11-INBS-0012), GLOMICAVE (H2020-EU.2.1.4 DO: I10.3030/952908) and GPR Bordeaux Plant Sciences in the framework of the IdEX Bordeaux University 'Investments for the Future' program.

CONFLICT OF INTEREST

All authors declare that they have no conflict of interest related to this work.

DATA AVAILABILITY STATEMENT

All relevant data can be found within the manuscript and its supporting materials.

SUPPORTING INFORMATION

Additional Supporting Information may be found in the online version of this article.

Appendix S1. Model in sbml. Zenodo data repository. https://zenodo.org/record/8163589.

Figure S1. Relative Growth Rate (RGR) with time expressed in Growing Degree-Days (GDD) in a panel of eight fruit species.

Figure S2. Correlations between RGR_{max} and maximal contents of biomass compounds in a panel of eight fruit species.

Figure S3. Time-course of RGR and protein content in a panel of eight fruit species.

Figure S4. Hierarchical clustering analysis performed with fluxes and relative growth rate calculated at 30 stages of development in a panel of eight fruit species.

Figure S5. Time-course of overall and redox fluxes in a panel of eight fruit species.

Figure S6. Time-course of fluxes involved in nitrogen metabolism in a panel of eight fruit species.

Figure S7. Alkaloids: flux and corresponding accumulated amount.

Figure S8. Growth and fluxes to set up virtual experiments.

Figure S9. High flux values for the 12 groups of outfluxes in virtual experiments.

Figure S10. Selection of 96 virtual experiments based on the mean of total biomass content.

Figure S11. Analysis of the experimental plan for 96 virtual experiments.

Figure S12. 3D-PCA with fluxes of the eight fruit species (Figure 4a) added with projection of the calculated fluxes for virtual experiments.

Figure S13. Clustering of fluxes calculated for both eight fruit species and 48 virtual experiments.

Figure S14. Image of correlation coefficients between 119 fluxes and RGR values at the fourth stage of development among 30 in a panel of 8 fruit species (values in Table S10).

Figure S15. RGR_{max} correlated with time to maturity in a panel of 16 fruit species.

Table S1. List of reactions in the metabolic model with their equations and properties.

Table S2. List of the metabolites in the metabolic model.

Table S3. Total phenolic compounds (TPC), nitrate and ammonium measured in the panel of eight fruit species.

Table S4. Mass balance from all biomass compounds at nine stages of development in the panel of eight fruit species.

Table S5. Fit applied on fruit metabolic data throughout development to calculate the corresponding rates in a panel of eight fruit species.

Table S6. Fluxes calculated at 30 stages of development in a panel of eight fruit species and 96 virtual experiments.

Table S7. Summary and loadings of PCA performed on flux data in a panel of eight fruit species.

Table S8. Nitrate reductase activity measured in a panel of eight fruit species.

Table S9. Virtual fruits experiments at 30 developmental stages with a fractional factorial plan including 12 factors at two levels (low and high).

Table S10. Correlation coefficients between 119 fluxes and RGR values at the fourth stage of development among 30 in a panel of 8 fruit species.

REFERENCES

Alonso-Blanco, C., Aarts, M.G.M., Bentsink, L., Keurentjes, J.J.B., Reymond, M., Vreugdenhil, D. *et al.* (2009) What has natural variation taught us about plant development, physiology, and adaptation? *The Plant Cell*, **21** (7), 1877–1896. Available from: https://doi.org/10.1105/tpc.109.068114

Arendt, J. (1997) Adaptive intrinsic growth rates: an integration across taxa. *The Quarterly Review of Biology*, **72**, 149–177. Available from: https://doi.org/10.1086/419764

Bagheri, M., Bushehri, A.A.S., Hassandokht, M.R. & Naghavi, M.R. (2017) Evaluation of solasonine content and expression patterns of SGT1 gene in different tissues of two Iranian eggplant (*Solanum melongena* L.) genotypes. *Food Technology and Biotechnology*, **55**(2), 236–242. Available from: https://doi.org/10.17113/ftb.55.02.17.4883

Barbero, G.F., Liazid, A., Azaroual, L., Palma, M. & Barroso, C.G. (2016) Capsaicinoid contents in peppers and pepper-related spicy foods. *International Journal of Food Properties*, **19**(3), 485–493. Available from: https://doi.org/10.1080/10942912.2014.968468

Beauvoit, B., Belouah, I., Bertin, N., Cakpo, C.B., Colombié, S., Dai, Z. *et al.* (2018) Putting primary metabolism into perspective to obtain better fruits. *Annals of Botany*, **122**(1), 1–21. Available from: https://doi.org/10.1093/aob/mcy057

Bekaert, M., Edger, P.P., Hudson, C.M., Pires, J.C. & Conant, G.C. (2012) Metabolic and evolutionary costs of herbivory defense: systems biology of glucosinolate synthesis. *New Phytologist*, **196**(2), 596–605. Available from: https://doi.org/10.1111/j.1469-8137.2012.04302.x

Belouah, I., Nazaret, C., Pétriacq, P., Prigent, S., Bénard, C., Mengin, V. *et al.* (2019) Modeling protein destiny in developing fruit. *Plant Physiology*, **180**, 1709–1724. Available from: https://doi.org/10.1104/pp.19.00086

Biais, B., Bénard, C., Beauvoit, B., Colombié, S., Prodhomme, D., Ménard, G. *et al.* (2014) Remarkable reproducibility of enzyme activity profiles in tomato fruits grown under contrasting environments provides a roadmap for studies of fruit metabolism. *Plant Physiology*, **164**(3), 1204–1221. Available from: https://doi.org/10.1104/pp.113.231241

Byrne, D., Raseira, M.C.B., Bassi, D., Piagnani, M.C., Gasic, K., Reighard, G.L. *et al.* (2012) Peach. In: Badenes, M.L. & Byrne, D.H. (Eds.) *Fruit breeding*, 1st edition. New York: Springer Science+Business Media, pp. 505–570. Available from: https://doi.org/10.1007/978-1-4419-0763-9_14

Cakpo, C.B., Vercambre, G., Baldazzi, V., Roch, L., Dai, Z., Valsesia, P. *et al.* (2020) Model-assisted comparison of sugar accumulation patterns in ten fleshy fruits highlights differences between herbaceous and woody species. *Annals of Botany*, **126**(3), 455–470. Available from: https://doi.org/10.1093/aob/mcaa082

Carillo, P., Kyriacou, M.C., el-Nakhel, C., Pannico, A., dell'Aversana, E., D'Amelia, L. *et al.* (2019) Sensory and functional quality characterization of protected designation of origin "Piennolo del Vesuvio" cherry tomato landraces from Campania-Italy. *Food Chemistry*, **292**, 166–175. Available from: https://doi.org/10.1016/j.foodchem.2019.04.056

Carranca, C., Brunetto, G. & Tagliavini, M. (2018) Nitrogen nutrition of fruit trees to reconcile productivity and environmental concerns. *Plants (Basel, Switzerland)*, **7**(1), 4. Available from: https://doi.org/10.3390/plants7010004

Chamizo-Ampudia, A., Sanz-Luque, E., Llamas, A., Galvan, A. & Fernandez, E. (2017) Nitrate reductase regulates plant nitric oxide homeostasis. *Trends in Plant Science*, **22**(2), 163–174. Available from: https://doi.org/10.1016/j.tplants.2016.12.001

Chen, Z., Deng, H., Xiong, B., Li, S., Yang, L., Yang, Y. *et al.* (2022) Rootstock effects on anthocyanin accumulation and associated biosynthetic gene expression and enzyme activity during Fruit development and ripening of blood oranges. *Agriculture*, **12**, 342. Available from: https://doi.org/10.3390/agriculture12030342

Chevalier, C., Nafati, M., Mathieu-Rivet, E., Bourdon, M., Frangne, N., Cheniclet, C. *et al.* (2011) Elucidating the functional role of endoreduplication in tomato fruit development. *Annals of Botany*, **107**(7), 1159–1169. Available from: https://doi.org/10.1093/aob/mcq257

Clark, T.J., Guo, L., Morgan, J. & Schwender, J. (2020a) Modeling plant metabolism: from network reconstruction to mechanistic models. *Annual Review of Plant Biology*, **71**(1), 303–326. Available from: https://doi.org/10.1146/annurev-arplant-050718-100221

Colombié, S., Beauvoit, B., Nazaret, C., Bénard, C., Vercambre, G., le Gall, S. *et al.* (2017) Respiration climacteric in tomato fruits elucidated by constraint-based modelling. *New Phytologist*, **213**(4), 1726–1739. Available from: https://doi.org/10.1111/nph.14301

Colombié, S., Nazaret, C., Bénard, C., Biais, B., Mengin, V., Solé, M. *et al.* (2015) Modelling central metabolic fluxes by constraint-based optimization reveals metabolic reprogramming of developing *Solanum lycopersicum* (tomato) fruit. *The Plant Journal*, **81**(1), 24–39. Available from: https://doi.org/10.1111/tpj.12685

Cope, O.L., Keefover-Ring, K., Kruger, E.L. & Lindroth, R.L. (2021) Growth–defense trade-offs shape population genetic composition in an iconic forest tree species. *Proceedings of the National Academy of Sciences of the United States of America*, **118**(37), e2103162118. Available from: https://doi.org/10.1073/pnas.2103162118

Corleto, K.A., Singh, J., Jayaprakasha, G.K. & Patil, B.S. (2019) A sensitive HPLC-FLD method combined with multivariate analysis for the determination of amino acids in l-citrulline rich vegetables. *Journal of Food and Drug Analysis*, **27**(3), 717–728. Available from: https://doi.org/10.1016/j.jfda.2019.04.001

Dai, Z., Wu, H., Baldazzi, V., van Leeuwen, C., Bertin, N., Gautier, H. *et al.* (2016) Inter-species comparative analysis of components of soluble sugar concentration in fleshy fruits. *Frontiers in Plant Science*, **7**, 649. Available from: https://doi.org/10.3389/fpls.2016.00649

Davison, J. (1958) Organ metabolism in mature mammals as the product of allometric mass and rate. *The American Naturalist*, **92**(863), 105–110. Available from: https://doi.org/10.1086/282016

Detto, M. & Xu, X. (2020) Optimal leaf life strategies determine $V_{c,max}$ dynamic during ontogeny. *New Phytologist*, **228**(1), 361–375. Available from: https://doi.org/10.1111/nph.16712

Elser, J., Sterner, R.W., Gorokhova, E., Fagan, W.F., Markow, T.A. & Cotner, J.B. (2000) Biological stoichiometry from genes to ecosystems. *Ecology Letters*, **3** (6), 540–550. Available from: https://doi.org/10.1111/j.1461-0248.2000.00185.x

Fang, C., Fernie, A. & Luo, J. (2018) Exploring the diversity of plant metabolism. *Trends in Plant Science*, **24**, 83–98. Available from: https://doi.org/10.1016/j.tplants.2018.09.006

Farinati, S., Forestan, C., Canton, M., Galla, G., Bonghi, C. & Varotto, S. (2021) Regulation of Fruit growth in a peach slow ripening phenotype. *Genes*, **12**(4), 482. Available from: https://doi.org/10.3390/genes12040482

Fenn, M.A. & Giovannoni, J.J. (2021) Phytohormones in fruit development and maturation. *The Plant Journal*, **105**(2), 446–458. Available from: https://doi.org/10.1111/tpj.15112

Friedman, M. (2015) Chemistry and anticarcinogenic mechanisms of glycoalkaloids produced by eggplants, potatoes, and tomatoes. *Journal of Agricultural and Food Chemistry*, **63**(13), 3323–3337. Available from: https://doi.org/10.1021/acs.jafc.5b00818

Friedman, M. & Levin, C.E. (1995) Alpha-tomatine content in tomato and tomato products determined by HPLC with pulsed amperometric detection. *Journal of Agricultural and Food Chemistry*, **43**(6), 1507–1511. Available from: https://doi.org/10.1021/jf00054a017

Gibeaut, D.M., Whiting, M.D. & Einhorn, T. (2017) Time indices of multiphasic development in genotypes of sweet cherry are similar from dormancy to cessation of pit growth. *Annals of Botany*, **119**(3), 465–475. Available from: https://doi.org/10.1093/aob/mcw232

Gibon, Y., Blaesing, O.E., Hannemann, J., Carillo, P., Höhne, M., Hendriks, J.H.M. *et al.* (2004) A robot-based platform to measure multiple enzyme activities in Arabidopsis using a set of cycling assays: comparison of changes of enzyme activities and transcript levels during diurnal cycles and in prolonged darkness. *The Plant Cell*, **16**(12), 3304–3325. Available from: https://doi.org/10.1105/tpc.104.025973

Gómez-Fernández, A. & Milla, R. (2022) How seeds and growth dynamics influence plant size and yield: integrating trait relationships into ontogeny. *Journal of Ecology*, **110**(11), 2684–2700. Available from: https://doi.org/10.1111/1365-2745.13979

Hamed, M., Kalita, D., Bartolo, M.E. & Jayanty, S.S. (2019) Capsaicinoids, polyphenols and antioxidant activities of *Capsicum annuum*: comparative study of the effect of ripening stage and cooking methods. *Antioxidants*, **8**(9), 364. Available from: https://doi.org/10.3390/antiox8090364

Hancock, J.T. (2019) Considerations of the importance of redox state for reactive nitrogen species action. *Journal of Experimental Botany*, **70**(17), 4323–4331. Available from: https://doi.org/10.1093/jxb/erz067

Hashemi, S., Laitinen, R. & Nikoloski, Z. (2023) Models and molecular mechanisms for trade-offs in the context of metabolism. *Molecular Ecology*, 1–11. Available from: https://doi.org/10.1111/mec.16879

He, Z., **Webster, S.** & **He, S.Y.** (2022) Growth–defense trade-offs in plants. *Current Biology*, **32**(12), R634–R639. Available from: https://doi.org/10.1016/j.cub.2022.04.070

Holzhütter, H.-G. (2004) The principle of flux minimization and its application to estimate stationary fluxes in metabolic networks. *European Journal of Biochemistry*, **271**(14), 2905–2922. Available from: https://doi.org/10.1111/j.1432-1033.2004.04213.x

Hoyos García, D., **Osorio, J.G.M.**, **Ardila, H.**, **Ríos, A.**, **Londoño, G.A.C.** & **Villegas, S.** (2012) Growing degree days accumulation in a cucumber (*Cucumis sativus* L.) crop grown in an aeroponic production model. *Revista - Facultad Nacional de Agronomía Medellín*, **65**(1), 6389–6398.

Huxley, J.S. & **Teissier, G.** (1936) Terminology of relative growth. *Nature*, **137**(3471), 780–781. Available from: https://doi.org/10.1038/137780b0

Jacob, D., **Deborde, C.** & **Moing, A.** (2020) BioStatFlow -statistical analysis workflow for "omics" data. *arXiv*. Available from: https://doi.org/10.48550/arXiv.2007.04599

Junker, B.H., **Lonien, J.**, **Heady, L.E.**, **Rogers, A.** & **Schwender, J.** (2007) Parallel determination of enzyme activities and in vivo fluxes in *Brassica napus* embryos grown on organic or inorganic nitrogen source. *Phytochemistry*, **68**(16–18), 2232–2242. Available from: https://doi.org/10.1016/j.phytochem.2007.03.032

Karasov, T.L., **Chae, E.**, **Herman, J.J.** & **Bergelson, J.** (2017) Mechanisms to mitigate the trade-off between growth and defense. *The Plant Cell*, **29**(4), 666–680. Available from: https://doi.org/10.1105/tpc.16.00931

Kołton, A., **Wojciechowska, R.** & **Leja, M.** (2012) The effect of various light conditions and different nitrogen forms on nitrogen metabolism in pepper fruits. *Folia Horticulturae*, **24**, 153–160. Available from: https://doi.org/10.2478/v10245-012-0019-8

Lang, C.P., **Merkt, N.** & **Zoerb, C.** (2018) Different nitrogen (N) forms affect responses to N form and N supply of rootstocks and grafted grapevines. *Plant Science*, **277**, 311–321. Available from: https://doi.org/10.1016/j.plantsci.2018.10.004

Li, L., **Nelson, C.J.**, **Trösch, J.**, **Castleden, I.**, **Huang, S.** & **Millar, A.H.** (2017) Protein degradation rate in *Arabidopsis thaliana* leaf growth and development. *The Plant Cell*, **29**(2), 207–228. Available from: https://doi.org/10.1105/tpc.16.00768

Liang, Y., **Liu, H.J.**, **Yan, J.** & **Tian, F.** (2021) Natural variation in crops: realized understanding, continuing promise. *Annual Review of Plant Biology*, **72**(1), 357–385. Available from: https://doi.org/10.1146/annurev-arplant-080720-090632

Liu, X., **Robinson, P.W.**, **Madore, M.A.**, **Witney, G.W.** & **Arpaia, M.L.** (1999) 'Hass' avocado carbohydrate fluctuations. II. Fruit growth and ripening. *Journal of the American Society for Horticultural Science*, **124**(6), 676–681. Available from: https://doi.org/10.21273/JASHS.124.6.676

Lu, Z.J. & **Neumann, P.M.** (1998) Water-stressed maize, barley and rice seedlings show species diversity in mechanisms of leaf growth inhibition. *Journal of Experimental Botany*, **49**(329), 1945–1952. Available from: https://doi.org/10.1093/jexbot/49.329.1945

Marmiesse, L., **Peyraud, R.** & **Cottret, L.** (2015) FlexFlux: combining metabolic flux and regulatory network analyses. *BMC Systems Biology*, **9**(1), 93. Available from: https://doi.org/10.1186/s12918-015-0238-z

Marra, F.P., **Inglese, P.**, **DeJong, T.M.** & **Johnson, R.S.** (2002) Thermal time requirement and harvest time forecast for peach cultivars with different FRUIT development periods. *Acta Horticulturae*, **592**, 523–529. Available from: https://doi.org/10.17660/ActaHortic.2002.592.70

Mathieu-Rivet, E., **Gévaudant, F.**, **Sicard, A.**, **Salar, S.**, **do, P.T.**, **Mouras, A.** ***et al.*** (2010) Functional analysis of the anaphase promoting complex activator CCS52A highlights the crucial role of endo-reduplication for fruit growth in tomato. *The Plant Journal*, **62**(5), 727–741. Available from: https://doi.org/10.1111/j.1365-313X.2010.04198.x

Mauceri, A., **Bassolino, L.**, **Lupini, A.**, **Badeck, F.**, **Rizza, F.**, **Schiavi, M.** ***et al.*** (2020) Genetic variation in eggplant for nitrogen use efficiency under contrasting NO_3^- supply. *Journal of Integrative Plant Biology*, **62**(4), 487–508. Available from: https://doi.org/10.1111/jipb.12823

Menary, R.C. & **Jones, R.H.** (1972) Nitrate accumulation and reduction in papaw fruits. *Australian Journal of Biological Sciences*, **25**(3), 531–542. Available from: https://doi.org/10.1071/bi9720531

Mennella, G., **Lo Scalzo, R.**, **Fibiani, M.**, **D'Alessandro, A.**, **Francese, G.**, **Toppino, L.** ***et al.*** (2012) Chemical and bioactive quality traits during fruit ripening in eggplant (*S. melongena* L.) and allied species. *Journal of Agricultural and Food Chemistry*, **60**(47), 11821–11831. Available from: https://doi.org/10.1021/jf3037424

Morata, J., **Béjar, S.**, **Talavera, D.**, **Riera, C.**, **Lois, S.**, **de Xaxars, G.M.** ***et al.*** (2013) The relationship between gene isoform multiplicity, number of exons and protein divergence. *PLoS One*, **8**(8), e72742. Available from: https://doi.org/10.1371/journal.pone.0072742

Moreno, S., **Canales, J.**, **Hong, L.**, **Robinson, D.**, **Roeder, A.H.K.** & **Gutiérrez, R.A.** (2020) Nitrate defines shoot size through compensatory roles for endoreplication and cell division in *Arabidopsis thaliana*. *Current Biology*, **30**(11), 1988–2000.e3. Available from: https://doi.org/10.1016/j.cub.2020.03.036

Ohyama, K., **Okawa, A.**, **Moriuchi, Y.** & **Fujimoto, Y.** (2013) Biosynthesis of steroidal alkaloids in Solanaceae plants: involvement of an aldehyde intermediate during C-26 amination. *Phytochemistry*, **89**, 26–31. Available from: https://doi.org/10.1016/j.phytochem.2013.01.010

Ohyama, T. (2010) Nitrogen as a major essential element of plants. In: Ohyama, T. & Sueyoshi, K. (Eds.) *Nitrogen assimilation in plants*. Kerala: Research Singpot, pp. 1–18.

Oikawa, A., **Otsuka, T.**, **Nakabayashi, R.**, **Jikumaru, Y.**, **Isuzugawa, K.**, **Murayama, H.** ***et al.*** (2015) Metabolic profiling of developing pear fruits reveals dynamic variation in primary and secondary metabolites, including plant hormones. *PLoS One*, **10**(7), e0131408. Available from: https://doi.org/10.1371/journal.pone.0131408

Perez-Roman, E., **Borredá, C.**, **Tadeo, F.R.** & **Talon, M.** (2022) Transcriptome analysis of the pulp of citrus fruitlets suggests that domestication enhanced growth processes and reduced chemical defenses increasing palatability. *Frontiers in Plant Science*, **13**, 982683. Available from: https://doi.org/10.3389/fpls.2022.982683

Poorter, H. & **Bergkotte, M.** (1992) Chemical composition of 24 wild species differing in relative growth rate. *Plant, Cell & Environment*, **15**(2), 221–229. Available from: https://doi.org/10.1111/j.1365-3040.1992.tb01476.x

Roch, L., **Dai, Z.**, **Gomès, E.**, **Bernillon, S.**, **Wang, J.**, **Gibon, Y.** ***et al.*** (2019) Fruit salad in the lab: comparing botanical species to help deciphering fruit primary metabolism. *Frontiers in Plant Science*, **10**, 836. Available from: https://doi.org/10.3389/fpls.2019.00836

Roch, L., **Prigent, S.**, **Klose, H.**, **Cakpo, C.B.**, **Beauvoit, B.**, **Deborde, C.** ***et al.*** (2020) Biomass composition explains fruit relative growth rate and discriminates climacteric from non-climacteric species. *Journal of Experimental Botany*, **71**(19), 5823–5836. Available from: https://doi.org/10.1093/jxb/eraa302

Ruiz, J.M. & **Romero, L.** (2002) Relationship between potassium fertilisation and nitrate assimilation in leaves and fruits of cucumber (*Cucumis sativus*) plants. *Annals of Applied Biology*, **140**(3), 241–245. Available from: https://doi.org/10.1111/j.1744-7348.2002.tb00177.x

Ruuska, S.A., **Schwender, J.** & **Ohlrogge, J.B.** (2004) The capacity of green oilseeds to utilize photosynthesis to drive biosynthetic processes. *Plant Physiology*, **136**(1), 2700–2709. Available from: https://doi.org/10.1104/pp.104.047977

Soubeyrand, E., **Colombié, S.**, **Beauvoit, B.**, **Dai, Z.**, **Cluzet, S.**, **Hilbert, G.** ***et al.*** (2018) Constraint-based modeling highlights cell energy, redox status and α-ketoglutarate availability as metabolic drivers for anthocyanin accumulation in grape cells under nitrogen limitation. *Frontiers in Plant Science*, **9**, 421. Available from: https://doi.org/10.3389/fpls.2018.00421

Subbaiah, C.C. & **Balasimha, D.** (1983) Nitrate reductase activity during ontogeny of the Fruit of cashew (*Anacardium occidentale* L.). *Functional Plant Biology*, **10**(1), 9–14. Available from: https://doi.org/10.1071/pp9830009

Sweetlove, L.J., **Obata, T.** & **Fernie, A.R.** (2014) Systems analysis of metabolic phenotypes: what have we learnt? *Trends in Plant Science*, **19**(4), 222–230. Available from: https://doi.org/10.1016/j.tplants.2013.09.005

Sweetlove, L.J., **Williams, T.C.R.**, **Cheung, C.Y.M.** & **Ratcliffe, R.G.** (2013) Modelling metabolic CO_2 evolution - a fresh perspective on respiration. *Plant Cell and Environment*, **36**(9), 1631–1640. Available from: https://doi.org/10.1111/pce.12105

Tandon, D.K. & **Kalra, S.K.** (1983) Changes in sugars, starch and amylase activity during development of mango fruit cv Dashehari. *Journal of Horticultural Science*, **58**(3), 449–453. Available from: https://doi.org/10.1080/00221589.1983.11515142

Teitel, D.C., **Arad, S.**, **Birnbaum, E.** & **Mizrahi, Y.** (1986) Nitrate reductase activity in tomato fruits grown in vivo and in vitro. *Plant Growth Regulation*, **4**(4), 357–362. Available from: https://doi.org/10.1007/BF00024935

Tong, H., **Küken, A.**, **Razaghi-Moghadam, Z.** & **Nikoloski, Z.** (2021) Characterization of effects of genetic variants via genome-scale metabolic modelling. *Cellular and Molecular Life Sciences*, **78**(12), 5123–5138. Available from: https://doi.org/10.1007/s00018-021-03844-4

Yin, H., **Li, B.**, **Wang, X.** & **Xi, Z.** (2020) Effect of ammonium and nitrate supplies on nitrogen and sucrose metabolism of cabernet sauvignon (*Vitis vinifera* cv.). *Journal of the Science of Food and Agriculture*, **100**(14), 5239–5250. Available from: https://doi.org/10.1002/jsfa.10574

Zhang, J., **Lv, J.**, **Dawuda, M.M.**, **Xie, J.**, **Yu, J.**, **Li, J.** ***et al.*** (2019) Appropriate ammonium-nitrate ratio improves nutrient accumulation and fruit quality in pepper (*Capsicum annuum* L.). *Agronomy*, **9**(11), 683. Available from: https://doi.org/10.3390/agronomy9110683

Zhang, L., **Zhu, S.H.**, **Chen, C.B.** & **Zhou, J.** (2011) Metabolism of endogenous nitric oxide during growth and development of apple fruit. *Scientia Horticulturae*, **127**(4), 500–506. Available from: https://doi.org/10.1016/j.scienta.2010.11.016

Zhu, W., **Zheng, Z.**, **Jiang, N.** & **Zhang, D.** (2018) A comparative analysis of the spatio-temporal variation in the phenologies of two herbaceous species and associated climatic driving factors on the Tibetan Plateau. *Agricultural and Forest Meteorology*, **248**, 177–184. Available from: https://doi.org/10.1016/j.agrformet.2017.09.021